Spout Eyes Formed by an Emerging Gas Plume at the Surface of a Slag-Covered Metal Melt

KIMITOSHI YONEZAWA and KLAUS SCHWERDTFEGER

This article deals with the spout eyes developing, at the surface of a metal melt, in the ladle during argon stirring. Cold model experiments involving a mercury bath with an oil layer as slag and industrial experiments on a 350 t steel ladle have been carried out. The eye geometry as measured with a video technique is highly dynamic. The time average of the free surface area and the time fraction of complete coverage have been determined and are represented with dimensionless correlations.

I. INTRODUCTION

THE region where the gas emerges during argon stirring in a metallurgical ladle is usually called a "spout." The spout can be covered with slag or it can be free of slag depending on the gas flow rate and the thickness of the slag layer. The latter state is established, by increasing the argon flow, when aluminum or other agents are added into the spout for the metallurgical correction of the melt. But before and after such additions, "soft bubbling" is carried out in usual practice with a covered spout. Naturally, the spout is the part of the free surface in the ladle where the agitation of slag and metal is strongest. Hence, it is the most important site for the slag/metal reactions in the metallurgical ladle treatment, and it is also the site for the undesired side reactions with air. There are many investigations on the hydrodynamics of gas plumes in liquids,[1,2,3] but only a few refer to the spout and most of these have been carried out with water as the model liquid.[4–8] The present article deals with the extension and dynamic behavior of "spout eyes," which are the open parts of the meniscus, uncovered by slag, during stirring with gas. The formation of spout eyes has not been studied previously, to our knowledge. Cold model experiments using mercury and silicon oil as metal and slag, respectively, and plant experiments involving a real 350 t steel ladle have been carried out.

II. EXPERIMENTAL METHOD OF LABORATORY MEASUREMENTS

The method used was that of observing the liquid surface with a video camera, combined with a data processing system. The experimental setup for the cold model experiments is sketched in Figure 1. The cylindrical vessel containing the mercury and silicon oil is made of PLEXIGLAS* and has an i.d. of 290 mm. The height of the mercury was chosen to be 225 mm in all the experiments. The thickness of the oil layer was varied between 3 and 30 mm. The silicon oil was grade AK 50 made by Wacker (Germany). It was colored blue with Sudanblue made by BASF (Germany). The densities of the liquids and gases are evident from Table I. The nozzle for injection of nitrogen is located at the center and its upper end is flush with the bottom of the vessel. The video camera was installed in the central axis of the vessel at a distance of 490 mm above the mercury/oil interface at rest. Two lamps of 60 W were used to illuminate the liquid surface, making a good contrast between mercury and oil.

The high-purity nitrogen was taken from a gas tank. The flow rates were measured *via* three flow meters with different ranges and pressure gages. The pressure-flow rate relationships of the flow meters were obtained prior to the experiments by calibration with a volumetric gas clock, which was placed behind the vessel to achieve a direct measurement of the gas volume at laboratory pressure and temperature. For this purpose, the vessel was closed, in the calibration procedure, with a tight lid equipped with an outlet tubing leading to the gas clock. Details are given elsewhere.[9]

The video camera is a CCD camera with normal objective of type CCD-88 made by Bischke (Germany). The recording system consists of the following parts: a central system, which is a Motorola 68000 processor (8 MHz) with 2 MB working storage and a VME-Bus unit with 8 slots; a video digitizer with 320 × 200 pixels, 4 Bit, and Lowres dissolution; and video storage with 4 Bit per pixel, 15 colors, and 40 MB. At the distance of the camera from the surface of 490 mm, the pixel size corresponds to 1.18 × 1.31 mm = 1.546 mm^2 on the surface. Two types of experiments were carried out. (1) The first was short time recording over about 0.8 seconds with 40 ms between consecutive pictures to investigate the dynamic behavior of the bath surface. In this case, the 20 pictures were kept stored in the working storage of the central system. (2) The second type involved long-time measurements over 62 minutes at a 6-second interval to determine time averages. The resulting 620 pictures were transferred to the video storage.

The digitizer divides the brightness range of the reflections in 15 classes and gives an own color to each class, with black for the brightest region. A photograph of the typical picture on the monitor is given in Figure 2. The large circle is the line of intersection between the silicon oil surface and the cylindrical wall of the vessel. The region outside of the circle is the inner wall of the vessel, which was covered with black paper (to avoid reflections) but still showed

*PLEXIGLAS is a trademark of Rohm & Haas Company, Philadelphia, PA.

KIMITOSHI YONEZAWA, formerly Scientist, Institut fur Allgemeine Metallurgie, Technische Universitat Clausthal, is with the Technical Administration and Planning Group, Nippon Steel Corporation, 6-3 Otemachi 2-chrome, Chiyoda-ku Tokyo, 100-71 Japan. KLAUS SCHWERDTFEGER, Professor, is with the Institute fur Allgemeine Metallurgie, Technische Universitat Clausthal, F Robert Koch Str. 42 D-38678 Clausthal-Zellerfeld, Germany.

Manuscript submitted February 20, 1998.

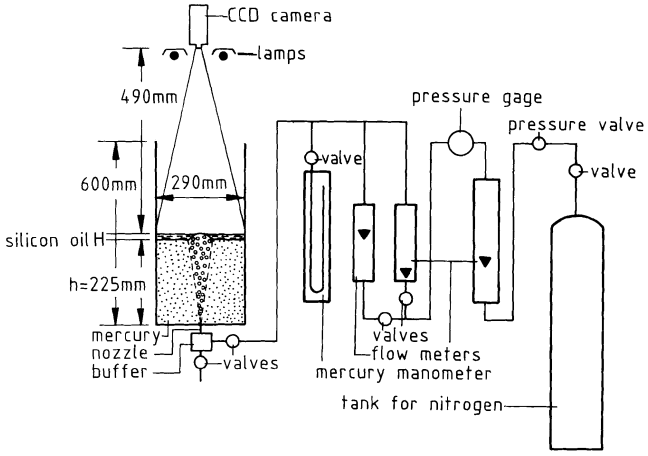

Fig. 1–Experimental setup used in the cold model experiments.

Table I. Physical Conditions and Densities of Liquids and Gases

Quantity	Mercury/Oil Model	350 t Steel Ladle
r_m, kg m^{23}	13600	7000
r_s, kg m^{23}	960	3000
$r_{g,b}$, kg m^{23}	1.429 (N_2)	0.876 (Ar)
T, 8C	20	1600
p_a, mm Hg	707	760
h, m	0.225	3.5

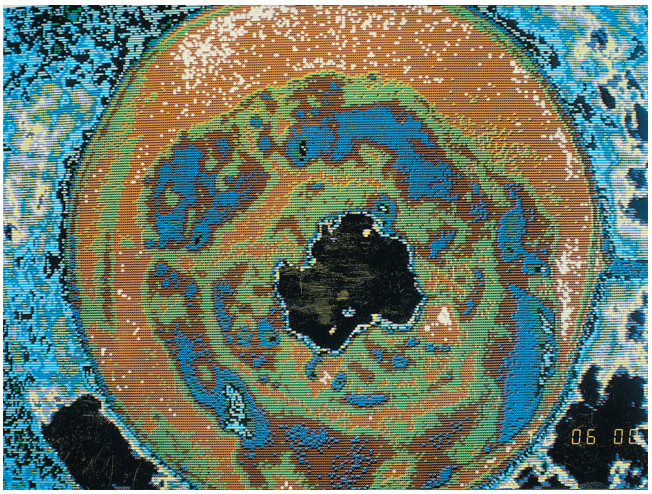

Fig. 2–Example for original video pictures. The circle is the line of intersection between the liquid meniscus and the cylindrical wall of the vessel. The black area within the circle is the open part (uncovered by slag) of the metal bath during nitrogen stirring.

reflecting areas due to oil stains made by splashes; the region inside is the liquid surface. The black area on the liquid (brightest region) is the open part of the surface, or ™eye,∫ where the slag is pushed away by the gas. The area of the eye and the number of the eyes, if the black area was subdivided into several black areas, were later evaluated using a data processing program. For the clarity of the text and of the diagrams, the definitions are given for the expressions spout, open spout area, and eye as used in the present article.

(1) Spout = region at surface in which the gas escapes into the environment during gas stirring of a metal bath. The spout may be completely covered by slag or partially or totally uncovered depending on the gas flow rate and thickness of the slag layer.

(2) Open spout area (or open metal area) = total region of metal surface, which is uncovered by slag,

(3) Eye = individual coherent uncovered region of an open spout. An open spout may have one or several eyes (Figure 3).

The symbols are explained in the List of Symbols.

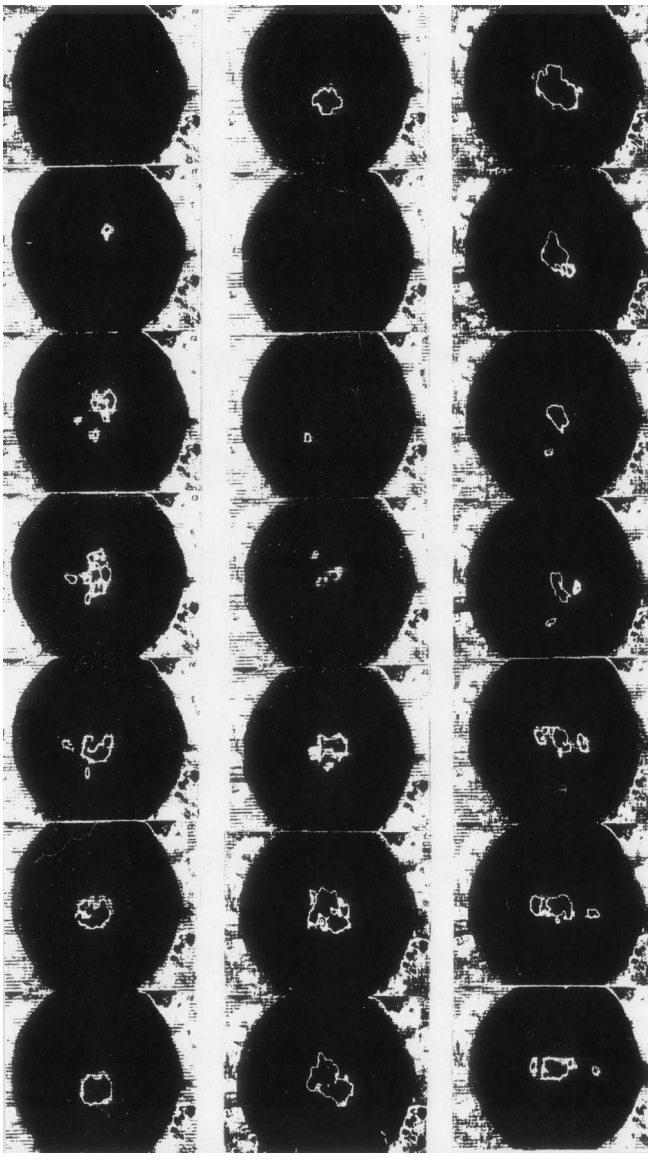

Fig. 3–Series of video pictures illustrating the dynamic behavior of the open spout. The pictures were made with the same electronic procedure as the picture in Fig. 2, but they were printed with a normal black and white printer, which was set so that only the rims of the eyes (white rim of black area in Figure 2) came out white. The time lapse between consecutive pictures is 40 ms. d = 1.0 mm, H = 20 mm, and Q_a = 0.6 m^3 h^{21}. Cold model experiment.

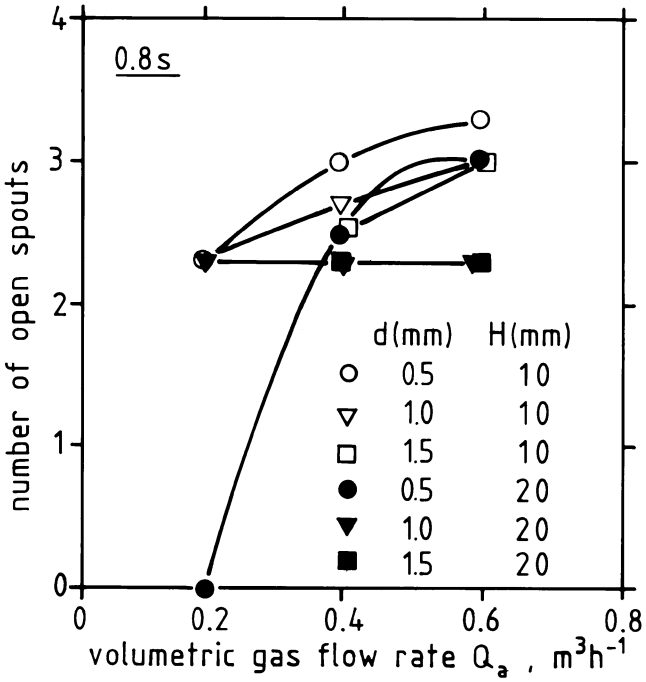

Fig. 4—Number of open spouts during 0.8 s (20 pictures). Cold model experiments.

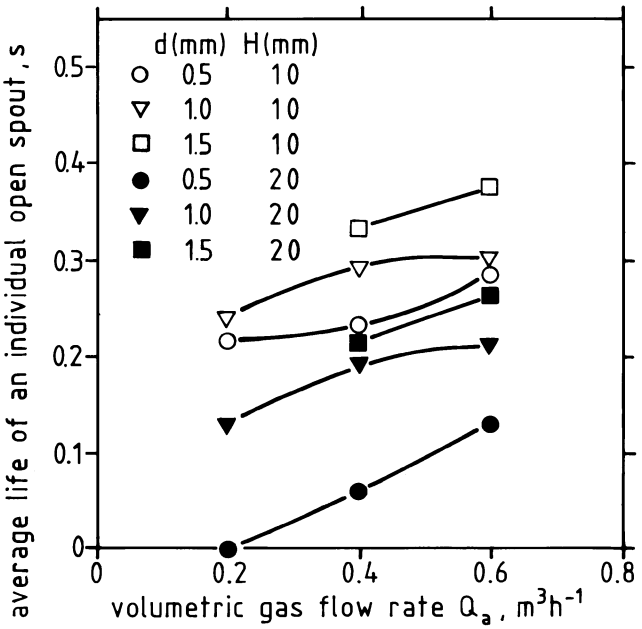

Fig. 5—Average life of an individual open spout. Cold model experiments.

III. DYNAMICAL BEHAVIOR OF OPEN SPOUT AREA (SHORT-TIME EXPERIMENTS)

Figure 3 shows a time series of surface pictures (time lapse: 40 ms). It is evident that there is a large fluctuation. There are pictures without open area, with open area of one single eye of varying size, and with open area of several eyes. Also, the position of the open area is not always exactly at the center of the vessel. Hence, the open bath area, looking rather steady with the bare eye, is highly dynamic on time resolution. This dynamic behavior is a consequence of the discontinuous gas discharge at the nozzle and of the subsequent disintegration into bubbles.

The life of a single open spout can be determined by counting the number of pictures where the same open area is seen and multiplication with 40 ms. Figures 4 and 5 show the average number of different open spouts developing in 0.8 seconds (20 pictures), as determined in three experiments, and the average life of an open spout, for three experiments. The number of open spouts is between two and four (if an open spout develops) in these series. This is in the same order of magnitude as the bubble frequency in a slag free mercury bath close to the interface, which has been measured in a previous study[1] using the electroresistivity probe technique. The life of an open spout is about 0.3 seconds at the low slag height of 10 mm, which is in the same order of magnitude as the residence time of a bubble in a mercury/oil (or mercury/water) interface.[10,11] With increasing slag height, the life of an eye becomes shorter and the frequency smaller. Such a behavior is quite reasonable since an increasing slag height acts against the formation of the open spout.

IV. LONG-TIME BEHAVIOR

Figure 6 gives an example for the size distribution of the open spout area as determined from 620 pictures taken in 62 minutes at 6-second intervals. Increasing gas flow rate shifts the spectra to larger sizes. Such spectra were deduced for several other experiments with different nozzle diameters *d* and slag heights *H*, indicating that they get broader with

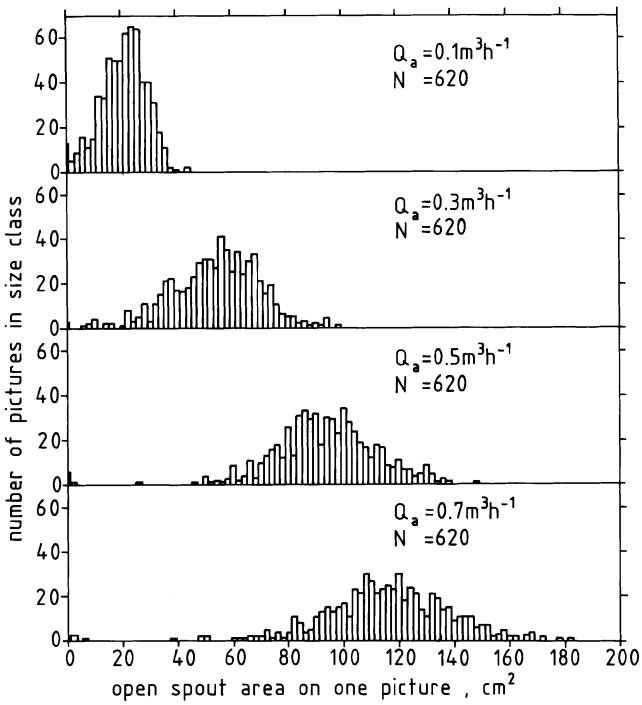

Fig. 6—Example for size distribution of open spout area. 620 pictures, time between consecutive pictures 6 s, total measuring time 62 min. d = 0.5 mm, and H = 5 mm. Cold model experiments.

increasing d and H, at the same gas flow rate. The other measured spectra are given elsewhere.[9]

The average quantities deduced from the measurements are collected in Table II. The average open spout area A values, obtained by summing up all the eye areas measured on the 620 pictures and division by 620, are shown in Figure 7 as a function of gas flow rate. It is evident that A increases with increasing gas flow rate and decreasing slag thickness. The influence of the nozzle orifice is not so clear. Whereas there is practically no difference between the data for the diameters of 1.0 and 1.5 mm, for 0.5 mm, the areas A are smaller particularly at the higher slag heights. The average number n of eyes per open spout varies between one and four in the range investigated. Figure 8 gives, as an example, the data for the nozzle with 1.0-mm diameter. The number n becomes larger with gas flow rate, and with increasing slag thickness, n first increases and then decreases again. Similar dependencies have been obtained for the other nozzle diameters of 0.5 and 1.5 mm.[9]

As may be expected, the spout can always be closed (no mercury visible) by slag, which happens at low gas flow rates and high slag thickness, and can always have open parts (all the pictures show mercury areas), which is so at high gas flow rates and thin slag layers. The number N_{nos} (of 620) of pictures with no open spout were counted (original data in Reference 9) and converted to the fraction of time f_{nos} without open spout (Table II). The dependency of f_{nos} on the gas flow rate and slag thickness is illustrated in Figure 9, for the nozzle with 1.0 mm.

It is to be noted that at very low slag height and high gas flow rate, the open bath area is considerably larger than the region normally called spout, where the gas bubbles escape. This is caused by the radial outward velocity at the metal surface, which pushes the slag away from the spout, thus producing a larger uncovered area than that taken by the emerging gas stream. We have also measured the radial plume width in the bulk of the liquid and the spout height (height of "dome") in the mercury/nitrogen system using the same geometry (liquid height, vessel diameter, and nozzle diameters) and can make a good comparison.[1,9] At the gas flow rate Q_a of 190 $cm^3\ s^{-1}$ and the nozzle diameter of 0.5 mm, the half-width $r_{1/2}$ of the bubble plume at a distance of 200 mm above the nozzle (=25 mm below the mercury surface at present bath height) was 22.8 mm,[1] which is equivalent to a cross-sectional area of 65 cm^2, taking the area as $(2r_{1/2})^2\pi$. For the same conditions, the half-width of the height profile of the dome was $r_{1/2} = 31.6$ mm,[9] yielding a dome (spout) area of 125 cm^2. On the other hand, the open metal area at a slag height of 3 mm (also called, in this text, open spout area) was 204 cm^2 according to the present study (Table II).

V. PLANT EXPERIMENTS

These experiments were carried out at the Yawata steelworks of Nippon Steel Corporation, using a 350 t ladle and LD steel of 0.02 pct C, 0.01 pct Si, 0.20 pct Mn, 0.015 pct P, and 0.010 pct S. The ladle diameter and bath height were 4.4 and 3.5 m, respectively, and the slag layer thickness was about 50 mm. The argon gas was introduced through an excentrically positioned sieve stone of 90-mm diameter at its upper end. In order to produce large open spouts, the gas flow rates were increased over the normal range (100 to 500

Table II. Experimental Data on Average Open Spout Characteristics as Determined in Cold Model Experiments

Slag Height, H (mm)	Gas Rate, Q_a ($m^3\ n^{-1}$)	Average Open Spout Area, A (cm^2)	Eyes/Open Spout, n	Fraction of Pictures Without Open Spout, f_{nos}
		d = 0.5 mm		
3	0.05	23.08	1.41	0
3	0.1	33.80	1.36	0
3	0.2	88.32	1.93	0.00161
3	0.3	136.39	1.86	0
3	0.4	168.61	1.90	0.00322
3	0.5	187.58	1.78	0
3	0.6	195.49	2.20	0
3	0.7	204.47	2.50	0
5	0.05	10.27	1.50	0.0274
5	0.1	20.05	1.70	0.0194
5	0.2	37.38	1.93	0.0242
5	0.3	52.95	2.06	0.00322
5	0.4	69.52	1.73	0.00161
5	0.5	93.10	2.12	0.00967
5	0.6	103.06	2.87	0
5	0.7	114.31	2.55	0
10	0.05	0.70	1.25	0.697
10	0.1	2.38	1.30	0.429
10	0.2	9.11	1.75	0.126
10	0.3	14.07	2.30	0.0629
10	0.4	21.11	2.45	0.0242
10	0.5	24.67	2.73	0.0306
10	0.6	28.20	2.35	0.0274
10	0.7	33.35	2.90	0.0048
15	0.05	0.05	1.05	0.905
15	0.1	0.23	1.29	0.795
15	0.2	2.37	1.78	0.319
15	0.3	3.45	1.78	0.324
15	0.4	6.08	2.20	0.182
15	0.5	12.03	2.61	0.108
15	0.6	12.75	2.20	0.0855
15	0.7	13.20	2.26	0.102
30	0.05	0	nos	1
30	0.1	0	nos	1
30	0.2	0	nos	1
30	0.3	0	nos	1
30	0.4	0.14	1.36	0.897
30	0.6	0.42	1.85	0.777
		d = 1.0 mm		
4	0.2	85.03	1.65	0
4	0.3	125.74	1.73	0.00806
4	0.4	140.90	1.74	0.00484
4	0.5	160.26	1.92	0
4	0.6	175.24	2.39	0
6	0.1	10.62	1.64	0.0645
6	0.2	49.36	2.08	0.00806
6	0.3	68.11	2.32	0.00806
6	0.4	88.46	2.45	0.00645
6	0.5	96.36	3.02	0.00806
6	0.6	102.42	3.40	0
10	0.2	11.13	2.02	0.150
10	0.4	30.03	2.31	0.0290
10	0.6	44.14	2.36	0.0338
10	0.7	54.87	2.82	0.0290
15	0.2	4.14	2.06	0.355
15	0.4	13.93	2.16	0.119

Table II. Continued

Slag Height, H (mm)	Gas Rate, Q_a (m^3 n^{-1})	Average Open Spout Area, A (cm^2)	Eyes/Open Spout, n	Fraction of Pictures Without Open Spout, f_{nos}
		d = 1.0 mm		
15	0.6	23.93	2.66	0.108
15	0.7	26.39	2.51	0.0903
20	0.2	1.47	1.75	0.555
20	0.4	4.84	2.16	0.356
20	0.6	10.44	2.58	0.221
20	0.7	13.54	2.52	0.134
30	0.2	0.08	1.69	0.947
30	0.4	0.57	1.74	0.776
30	0.6	1.55	1.88	0.627
		d = 1.5 mm		
5	0.4	100.03	3.14	0.0210
5	0.6	118.66	3.47	0
5	0.7	125.06	3.67	0
10	0.4	28.55	2.31	0.0339
10	0.6	38.06	2.71	0.0242
10	0.7	48.82	3.13	0.0161
15	0.4	10.87	2.29	0.192
15	0.6	22.23	2.82	0.0597
15	0.7	26.34	2.76	0.0484
20	0.4	3.83	1.99	0.419
20	0.6	11.01	2.34	0.194
20	0.7	14.22	2.76	0.121
30	0.4	0.42	1.50	0.815
30	0.6	1.56	2.24	0.639
30	0.7	2.91	2.07	0.523

nos = no open spout.

Nl min^{-1}). A photograph of two spouts is shown in Figure 10. Again, the video camera technique was applied to measure the area of the open spout.

Three experiments were carried out. The results are listed in Table III. Similarly as in the cold model studies, the open spout area increases with increasing gas flow (Figure 11).

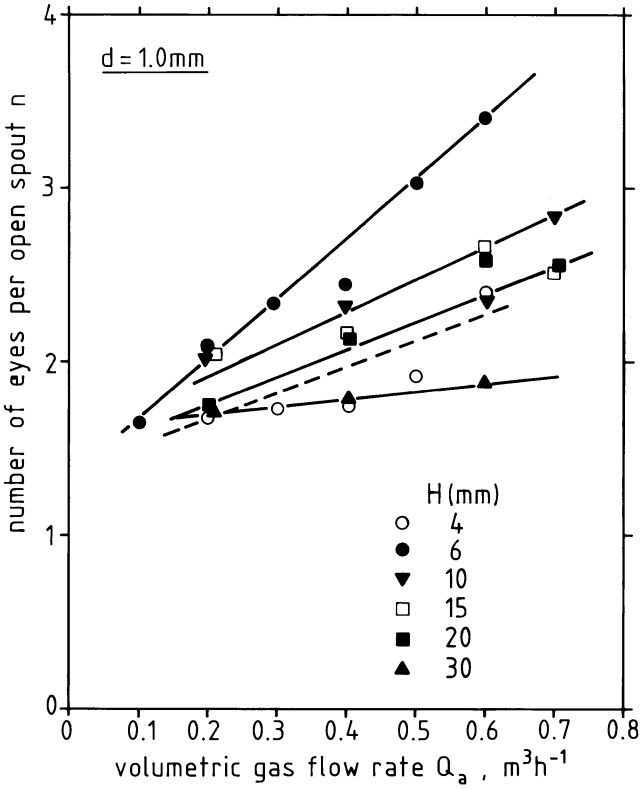

Fig. 8—Selected data on the subdivision of the open spout into several eyes. Cold model experiments.

VI. NONDIMENSIONAL ANALYSIS

It is probably impossible to describe the complex dynamic behavior of the open spout with mathematical modeling of the flow field in the three-phase system. Hence, the nondimensional analysis was applied to find the empirical laws governing the average open metal area A and the fraction of time f_{nos} with no open area. In principle, both quantities depend on the independent variables Q_a (or Q_b), H, d, h, g,

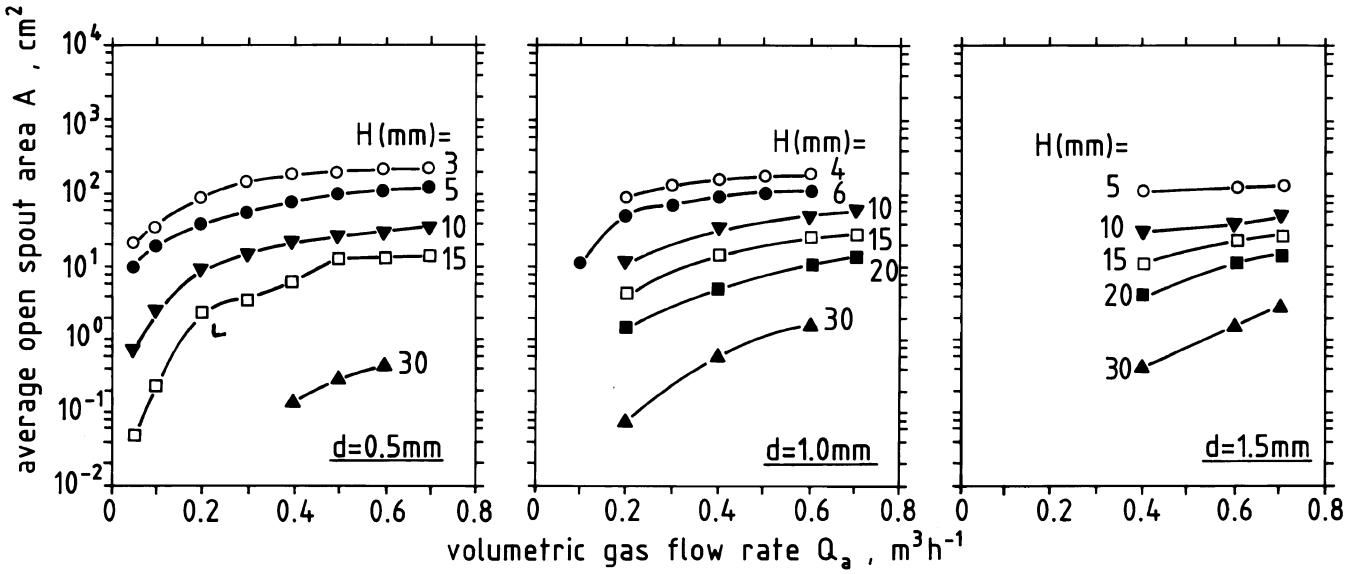

Fig. 7—Average area of open spout as a function of volumetric gas flow rate at constant values of slag thickness. Cold model experiments.

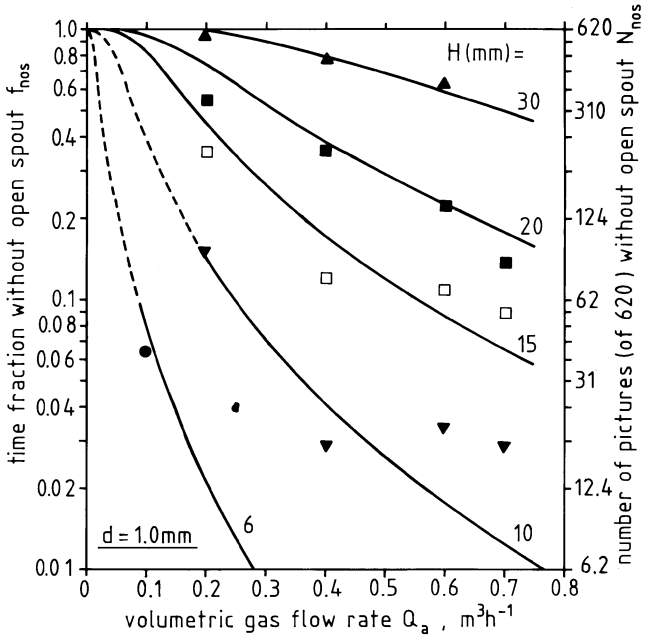

Fig. 9—Fraction of time or number of pictures (of 620) without open spout as a function of gas flow rate at constant values of slag thickness. Cold model experiments.

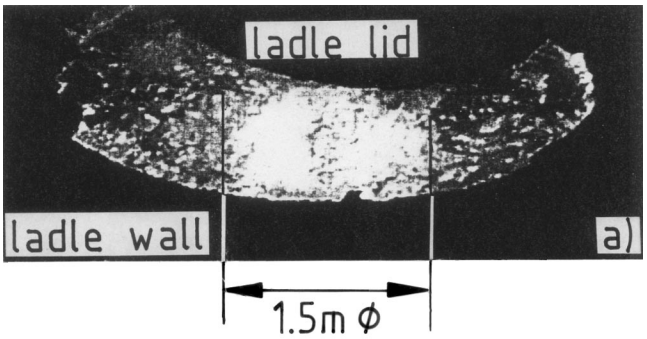

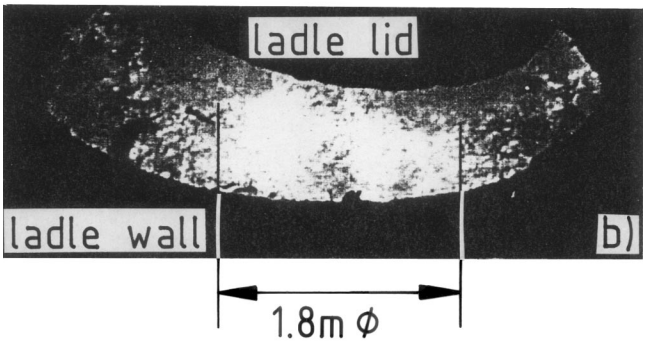

Fig. 10—Photograph of spout surface of argon stirred 350 t steel ladle. The spout appears to be oval because the picture is taken at an angle, but in reality the spout is round: (*a*) Q_o = 600 Nl min^{-1}, and (*b*) Q_o = 800 Nl min^{-1}.

p_a, ρ_m, ρ_s, $\rho_{g,a}$ (or $\rho_{g,b}$), η_m, η_s, η_g, σ_{ms}, σ_{mg}, and σ_{sg}. In the laboratory experiments, the materials (metal, slag, and gas) were not varied. Hence, the influence of the densities, viscosities, and surface tensions cannot be deduced and the density ratios, viscosity ratios, and nondimensional numbers

Table III. Open Spout Area in 350 t Steel Ladle during Argon Stirring

Experiment	Slag Height, H (mm)	Gas Rate, Q_0 (Nl min^{-1})	Open Spout Area, A (cm^2)
1	50	450	19,100
		600	20,600
		625	20,600
		625	20,100
		750	20,600
		350	15,800
2	50	600	17,700
		800	24,300
3	50	450	20,100
		600	21,600
		750	22,200

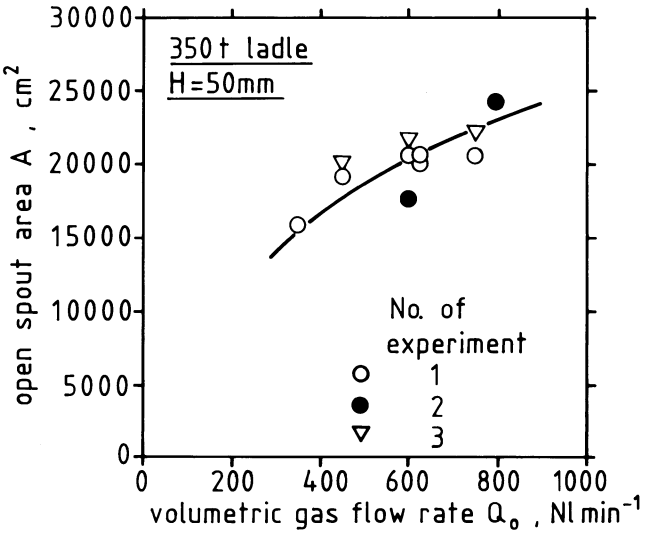

Fig. 11—Area of open spout in 350 t steel ladle stirred with argon as a function of gas flow rate.

involving interfacial energies have been omitted in the nondimensional correlations. Since in steelmaking the density ratios and viscosity ratios of metal and slag and the interfacial tensions are of the same order of size, the correlations determined with the mercury/oil system may not be too far off for predicting the spout characteristics in ladle metallurgy.

The nondimensional correlation for the open metal area can be taken to be between the quantities

$$\frac{A}{h^2}, \frac{Q_b^2}{gH^5}, \frac{H}{h}, \frac{d}{h}, \frac{p_a}{p_b} \qquad [1]$$

In order to find the functional relationship, the quantitiy A/h^2 was first plotted against the Froude number $Q_b^2/(gH^5)$ for the three experimental series with different d/h.[9] But in such plots, there is still a clear stratification of the experimental points for different slag thickness with A/h^2 increasing approximately proportional to H/h at given $Q_b^2/(gH^5)$. This effect indicates that $(A/h^2)(h/H)$ should be a sole function of $Q_b^2/(gH^5)$. Figure 12 shows $A/(hH) = (A/h^2)(h/H)$ plotted against $Q_b^2/(gH^5)$. Different equations were used to represent the data points for the nozzle with d = 0.5 mm or d = 1.0 and 1.5 mm.

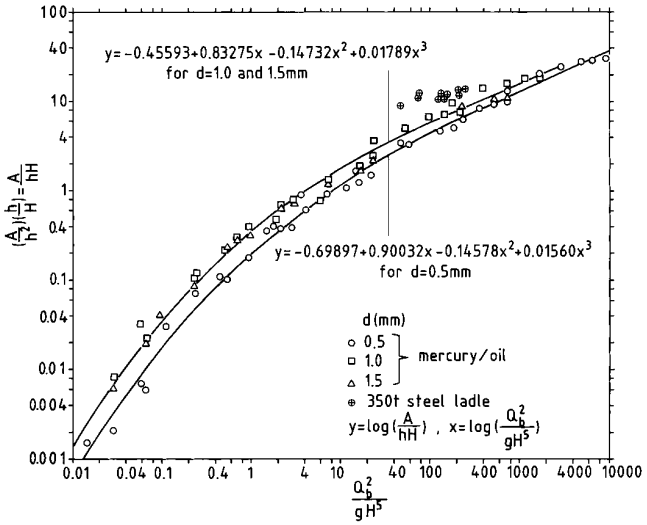

Fig. 12—Nondimensional representation of average area of open spout. Comparison of the experimental data with Eq. [2] and [3].

$$\log\left(\frac{A}{hH}\right) = -0.69897 + 0.90032\log\left(\frac{Q_b^2}{gH^5}\right) - 0.14578\left[\log\left(\frac{Q_b^2}{gH^5}\right)\right]^2 + 0.01560\left[\log\left(\frac{Q_b^2}{gH^5}\right)\right]^3 \quad \text{for } 0.01 < \frac{Q_b^2}{gH^5} < 10{,}000 \text{ and } d = 0.5 \text{ mm} \quad [2]$$

$$\log\left(\frac{A}{hH}\right) = -0.45593 + 0.83275\log\left(\frac{Q_b^2}{gH^5}\right) - 0.14732\left[\log\left(\frac{Q_b^2}{gH^5}\right)\right]^2 + 0.01789\left[\log\left(\frac{Q_b^2}{gH^5}\right)\right]^3 \quad \text{for } 0.01 < \frac{Q_b^2}{gH^5} < 2000 \text{ and } d = 0.1 \text{ and } 1.5 \text{ mm} \quad [3]$$

Included in Figure 12 are the results of the real size steel experiments, which are close to the correlations for the cold model experiments, but at somewhat higher $A/(hH)$. There can be several explanations for the deviation. Since the Froude number contains the slag thickness with the power 5, errors in slag thickness influence rather strongly the magnitude of $Q_b^2/(gH^5)$. That is, if H were 4 cm instead of the used 5 cm, the points for the steel experiments would be shifted to $Q_b^2/(gH^5)$ values larger by a factor of about 3 and would be located very close to the upper curve in Figure 12. The deviation may also be physically real originating from the fact that the nondimensional correlations [2] and [3] are not complete lacking the quantities p_a/p_b and d/h. In the ladle experiments, the pressure ratio p_a/p_b is smaller by a factor of about 2.6 than in the cold model experiments. In fact, it appears to be reasonable that a decreasing pressure ratio should increase the spout area because of the increase of the gas volume at the metal surface. The ratio d/h is 0.0022 and 0.0044 or 0.0066 in the cold model experiments for $d = 0.5$ or 1.0 and 1.5 mm, respectively, and 0.026 in the steel ladle experiments (taking the sieve stone diameter as d). The influence of nozzle diameter on the spout area is not clear from the present experiments, as has been mentioned. But it would not be unreasonable if the spout area increases somewhat with the nozzle diameter. Finally, a systematic measuring error may have existed in the steel experiments. It was difficult to distinguish between hot slag and liquid steel in the spout area. Hence, the total light area was taken to be open, which may not have been so. Anyway, it may be concluded that the agreement between the nondimensional data for the cold model experiments and for the steel ladle is rather satisfactory.

Similarly, the correlation for f_{nos}, in principle, will be between the quantities

$$f_{nos}, \frac{Q_b^2}{gH^5}, \frac{H}{h}, \frac{d}{h}, \frac{p_a}{p_b} \quad [4]$$

In order to deduce the functional relationship between f_{nos}, Q_b, and H, the Q_b values for specified f_{nos} values were read from the curves in Figure 9 (and in corresponding diagrams for $d = 0.5$ mm and $d = 1.5$ mm) and plotted against H. It was found that Q_b varies with H exponentially with the exponent of about 2, $Q_b \sim H^2$, for $f_{nos} = \text{const}$. Hence, using again $Q_b^2/(gH^5)$ and (H/h) as the nondimensional variables, the correlation should contain the combination $[(Q_b^2/(gH^5)](H/h) = Q_b^2/(gH^4h)$. Figure 13(a) shows f_{nos} as a function of $[(Qb^2/(gH^5)](H/h)$. The drawn curve is given by equation

$$\log f_{nos} = -1.91025 - 1.09553\log\left(\frac{Q_b^2}{gH^4h}\right) - 0.09360\left[\log\left(\frac{Q_b^2}{gH^4h}\right)\right]^2 + 0.019775\left[\log\left(\frac{Q_b^2}{gH^4h}\right)\right]^3 \quad \text{for } 0.001 < \frac{Q_b^2}{gH^4h} < 10 \quad [5]$$

The data points are represented quite well by expression [5] down to about $f_{nos} = 0.03$. The increasing scatter at low f_{nos} is natural in the logarithmic plot because the relative error of f_{nos} becomes infinity with f_{nos} (or N_{nos}) approaching zero. In Figure 13(b), the corresponding plot of $f_{os} = 1 - f_{nos}$ is shown. From these two diagrams, it can be deduced that below $Q_b^2/(gH^4h) = 0.001$, f_{nos} will be practically 1, and above $Q_b^2/(gH^4h) = 1$, f_{os} will be practically 1. That is, for conditions with $Q_b^2/(gH^4h) < 0.001$, there will (practically) never be an open area, and for conditions with $Q_b^2/(gH^4h) > 1$, there will (practically) always be an open area. It would be interesting to check these data in the real steel ladle because such criteria would be very useful to establish the conditions for secure soft bubbling (no open area) and secure aluminum addition (open area).

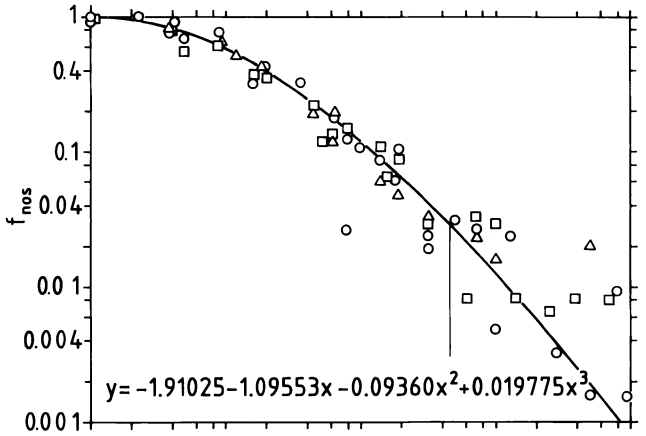

(*a*)

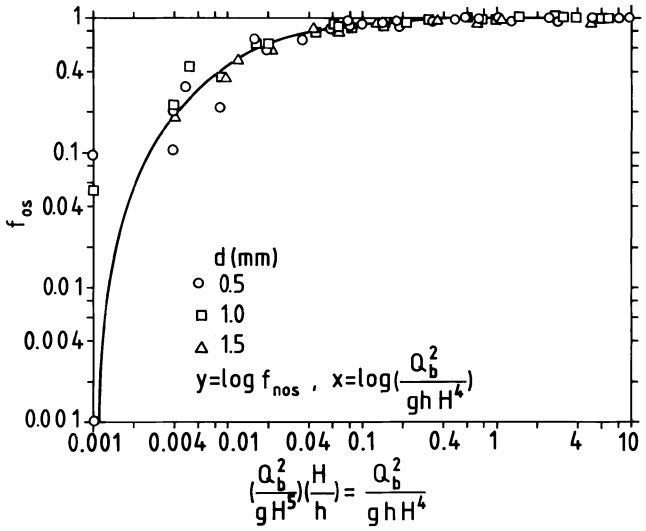

(*b*)

Fig. 13—(*a*) and (*b*) Nondimensional representation of time fraction without open spout (f_{nos}) and time fraction with open spout (f_{os}). Comparison of the experimental data with Eq. [5]. Cold model experiments.

VII. SUMMARY AND CONCLUSIONS

In the present work, the development of open spouts, that is, of spouts not covered by slag, during argon stirring of a liquid metal bath has been investigated with cold model experiments using mercury as metal and silicon oil as slag. The formation of the open spout is a very dynamic process with its size, number of individual eyes per open spout, and eye location highly fluctuating with time. Nondimensional correlations were established for the time average of the open area and the time fraction for existence of an open or a closed spout. Measurements in a real steel ladle during argon stirring confirm the correlation for the open spout area within the order of magnitude.

It appears that the formation of the open spout on a slag covered metal melt has not been investigated previously in a systematic way, although the matter is of considerable practical importance. Our study, however, does not clarify the subject completely because several parameters were not varied in the experiments, *viz.* metal height (or pressure ratio) and material properties. Hence, more work should be carried out to complement the derived nondimensional correlations.

ACKNOWLEDGMENTS

This work was sponsored by Deutsche Forschungsgemeinschaft under Grant No. Schw 176/22.

LIST OF SYMBOLS

A	"long time" average of open spout area (open metal area) $A = \Sigma_1^{620} A_i/620$
A_i	open spout area (of eyes) on one picture
H	height of slag layer
N	total number of pictures, $N = 620$
N_{eye}	total number of eyes, $N_{eye} = \Sigma_1^{620} N_i$
N_i	number of eyes on one picture
N_{nos}	number of pictures without open spout (nos = no open spout)
N_{os}	number of pictures with open spout (os = open spout), $N_{nos} + N_{os} = N = 620$
d	nozzle diameter
Q_o	gas flow rate at standard temperature and pressure
Q_a	volumetric gas flow rate at laboratory temperature and pressure (pressure is 707 mm Hg in Clausthal)
Q_b	volumetric gas flow rate at nozzle exit (bottom of vessel)
h	height of metal in vessel at rest
f_{nos}	fraction of time (or pictures) without open spout (open metal area), $f_{nos} = N_{nos}/620$
f_{os}	fraction of time (or pictures) with open spout (open metal area), $f_{os} = N_{os}/620$
g	gravitation constant
n	average number of eyes per open spout ($n = N_{eye}/N_{os}$)
p_a	ambient pressure
p_b	gas pressure at nozzle exit ($p_b = p_a + \rho_m gh + \rho_s H$)
ρ_m, ρ_s	densities of metal and slag phase
$\rho_{g,b}$, $\rho_{a,b}$	density of gas at nozzle exit (bottom of vessel) and at meniscus
η_m, η_s, η_g	viscosities of metal, slag, and gas phase
σ_{ms}, σ_{mg}, σ_{sg}	interfacial energies at metal/slag, metal/gas, and slag/gas interfaces

REFERENCES

1. K.-H. Tacke, H.-G. Schubert, D.-J. Weber, and K. Schwerdtfeger: *Metall. Trans. B*, 1985, vol. 16B, pp. 263-75.
2. A.H. Castillejos and J.K. Brimacombe: *Metall. Trans. B*, 1987, vol. 18B, pp. 659-71.
3. M.A.S.C. Castello-Branco and K. Schwerdtfeger: *Metall. Mater. Trans. B*, 1994, 25B, pp. 359-71.
4. E. Steinmetz and P.R. Scheller: *Stahl Eisen*, 1987, vol. 107(9), pp. 417-25.
5. V. Sahajwalla, A.H. Castillejos, and J.K. Brimacombe: *Metall. Trans. B*, 1990, vol. 21B, pp. 71-80.
6. Y. Matsukura: *CAMP-ISIJ*, 1991, vol. 4, p. 974.
7. Y. Higuchi: *CAMP-ISIJ*, 1991, vol. 4, p. 975.
8. Y. Iguchi and K.K. Brimacombe: *CAMP-ISIJ*, 1993, vol. 6, p. 1042.
9. K. Yonezawa: Dr. Ing. Dissertation, Technical University Clausthal, Clausthal-Zellerfeld, Germany, 1994.
10. G. Reiter and K. Schwerdtfeger: *Iron Steel Inst. Jpn. Int.*, 1992, vol. 32 (1), pp. 50-56.
11. G. Reiter and K. Schwerdtfeger: *Iron Steel Inst. Jpn. Int.*, 1992, vol. 32 (1), pp. 57-65.